

Modeling Tunnel Junctions for VCSELs: A Self-Consistent NEGF-DD Approach

*Original*

Modeling Tunnel Junctions for VCSELs: A Self-Consistent NEGF-DD Approach / Tibaldi, Alberto; Gullino, Alberto; Montoya, Jesus Gonzalez; Alasio, Matteo; Larsson, Anders; Debernardi, Pierluigi; Goano, Michele; Vallone, Marco; Ghione, Giovanni; Bellotti, Enrico; Bertazzi, Francesco. - ELETTRONICO. - (2020), pp. 67-68. ((Intervento presentato al convegno <https://ieeexplore.ieee.org/document/9217684> tenutosi a Online conference nel September 2020 [10.1109/NUSOD49422.2020.9217684]).

*Availability:*

This version is available at: 11583/2848459 since: 2020-10-14T16:50:08Z

*Publisher:*

IEEE

*Published*

DOI:10.1109/NUSOD49422.2020.9217684

*Terms of use:*

openAccess

This article is made available under terms and conditions as specified in the corresponding bibliographic description in the repository

*Publisher copyright*

IEEE postprint/Author's Accepted Manuscript

©2020 IEEE. Personal use of this material is permitted. Permission from IEEE must be obtained for all other uses, in any current or future media, including reprinting/republishing this material for advertising or promotional purposes, creating new collecting works, for resale or lists, or reuse of any copyrighted component of this work in other works.

(Article begins on next page)

# Modeling Tunnel Junctions for VCSELs: A Self-Consistent NEGF-DD Approach

Alberto Tibaldi<sup>\*†</sup>, Alberto Gullino<sup>\*</sup>, Jesús Gonzalez Montoya<sup>\*</sup>, Matteo Alasio<sup>\*</sup>, Anders Larsson<sup>‡</sup>, Pierluigi Debernardi<sup>†</sup>, Michele Goano<sup>\*†</sup>, Marco Vallone<sup>\*</sup>, Giovanni Ghione<sup>\*</sup>, Enrico Bellotti<sup>§</sup>, and Francesco Bertazzi<sup>\*†</sup>

<sup>\*</sup> Department of Electronics and Telecommunications, Politecnico di Torino, 10129 Turin, Italy

<sup>†</sup> CNR-IEIIT c/o Politecnico di Torino, 10129 Turin, Italy

<sup>‡</sup> Department of Microtechnology and Nanoscience, Chalmers University of Technology, SE-412 96 Göteborg, Sweden.

<sup>§</sup> Department of Electrical and Computer Engineering, Boston University, Boston, MA 02215, USA.

E-mail: alberto.tibaldi@polito.it

**Abstract**—In this work we investigate carrier transport in tunnel junctions for vertical-cavity surface-emitting lasers by a novel self-consistent simulation framework for semiconductor quantum devices. Based on a Poisson-drift-diffusion foundation, in this approach quantum features are described through a nonequilibrium Green’s function formalism. The simulator is validated through a comparison with experimental results.

## I. INTRODUCTION

Tunnel junctions (TJs) are very interesting in the optoelectronic devices whose performance are affected by the poor transport properties of holes. This is for example the case of vertical-cavity surface-emitting lasers (VCSELs), where TJs could allow to eliminate most of the  $p$ -doped regions, reducing the device resistance and improving both the VCSEL power consumption and modulation speed. Moreover, transverse current confinement could be engineerized through selective etching [1], [2] or wafer-fusion processes [3] replacing the critical wet oxidation fabrication step.

Even though a rigorous model of TJ-based (opto)electronic devices should describe the entangled interaction between the extended current-carrying states with the localized states involved in spontaneous/stimulated emission processes, the huge computational cost of a genuine quantum-kinetic approach applied to a whole device at present is prohibitive. This is why scientists developed *quantum-corrected* semiclassical models, where drift-diffusion pictures describe transport in the bulky regions, and local corrections are introduced where quantum effects are present [4], [5], [6], [7]. With reference to the quantum tunneling model proposed in the seminal work of Kane [8], local [9], [10] and non-local [11], [12] models have been successfully applied to silicon devices. However, their application to other material systems is quite debated for numerical stability issues [13], for their possible inadequacy in modeling forward-bias tunnel junctions [14], or for carrier generation saturation issues [15].

Still on the basis of the semiclassical-founded multiscale strategy, in this paper the Kane-like tunneling models are replaced with genuine quantum-kinetic computations performed with a non-equilibrium Green’s function (NEGF) solver and

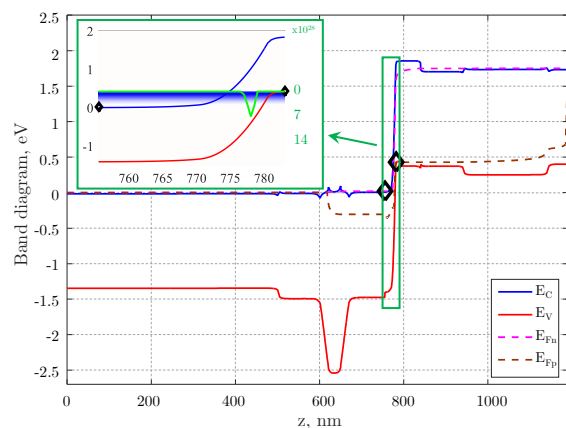


Fig. 1. Simulated band diagram of the device under analysis at 2.3 V bias. The conduction and valence band edges are indicated with solid blue and red curves, respectively. The electron and valence quasi-Fermi levels are indicated with dashed magenta and brown lines, respectively. The TJ is the  $np$  junction closed in the green rectangular box. The black diamond markers indicate the quasi-Fermi levels at the boundaries of the NEGF simulation window, which is magnified in the top-left inset. Here, the blue cloud indicates the energy-resolved total current, where dark blue indicates  $4 \times 10^4 \text{ A cm}^{-2} \text{ eV}^{-1}$  levels. Superimposed on it, one can find the estimated  $G_{\text{NEGF}}$  (green line), whose peak value is about  $7 \times 10^{28} \text{ cm}^{-3} \text{ s}^{-1}$ .

coupled self-consistently to drift-diffusion (DD). This technique is applied to a preliminary test structure for TJ-VCSELs, achieving good agreement with the experimental results.

## II. METHODOLOGY AND RESULTS

The DD equations are solved over the whole device, with a Scharfetter-Gummel discretization scheme to ensure numerical stability [16], [17]. Considering that the simplest band structure providing a reasonable description of band-to-band tunneling is a 4-band  $\mathbf{k} \cdot \mathbf{p}$  (including electrons, light and heavy holes, and split-off bands), the staggering computational cost allows to include in the Hamiltonian only the portion of the band diagram where quantum effects are relevant, which in this work is the tunnel junction. Open boundary conditions are enforced at the ending sections of the considered band diagram cuts, which are accounted for by means of boundary self-

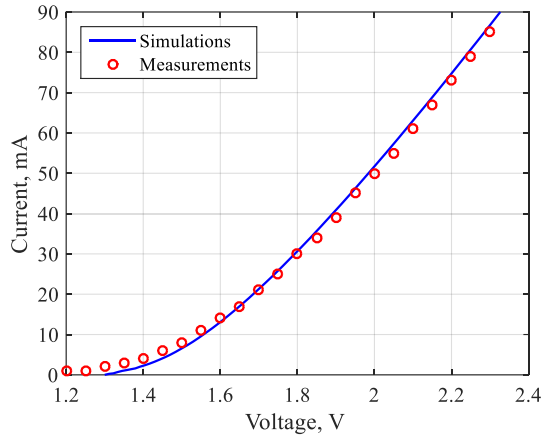


Fig. 2.  $VI$  characteristics of the device under study. Simulation and experimental results are reported with blue solid curves and red open bullets, respectively.

energies [18], [19]. These self-energies are computed assuming to have the contacts at equilibrium. This allows to describe the energy distribution of the injected charge with a Fermi-Dirac distribution, where the quasi-Fermi levels are those obtained from the DD solution, evaluated at the NEGF simulation window bounds.

The NEGF solver is coupled to the DD through a generation/recombination (GR) term  $G_{\text{NEGF}}$  computed as

$$G_{\text{NEGF}} = \frac{1}{q} \frac{\partial J_{n,\text{NEGF}}}{\partial z} = -\frac{1}{q} \frac{\partial J_{p,\text{NEGF}}}{\partial z}, \quad (1)$$

where  $q$  is the elementary charge, and  $J_{n,\text{NEGF}}$  ( $J_{p,\text{NEGF}}$ ) is the electron (hole) current density computed with NEGF. The DD and NEGF computations are repeated until self-consistent charge carrier Green's functions and DD band diagram are obtained.

This NEGF-DD approach has been applied to an AlGaAs-based device test structure designed at Chalmers University and grown by IQE. The material and doping profiles can be qualitatively inferred by the band diagram reported in Fig. 1. In more detail, most of the layers contain 12% Al molar fraction, with the exceptions of the GaAs substrate (the first 500 nm), the undoped layer (starting at about 870 nm, which would be replaced by the VCSEL active region), the top line contact, and the high Al-content oxide aperture (characterized by the deep valence band valley). The doping density is  $3 \times 10^{18}$  everywhere, except in the undoped region and in the  $n^{++}$  ( $2 \times 10^{19}$ ) and  $p^{++}$  ( $2 \times 10^{20}$ ) layers forming the tunnel junction.

The blue horizontal strip in the inset of Fig. 1 represents the total (electron plus hole) spectral current density. This is indicative of coherent transport, i.e., band-to-band tunneling. This result is specific to the buried tunnel junction considered here, as opposed to indirect semiconductors where phonon-assisted contributions are important [20], [21], or nanostructured TJs employed in multijunction solar cells, where an inelastic scattering process is needed to overcome energetic misalignments between the bound, quasibound, and continuum

states participating in the interband tunneling process [22], [23].

Fig. 2 shows the simulated (solid curve) and measured (circles)  $IV$  characteristics, where a  $6 \Omega$  series resistance was included to account for non-ideal contacts and substrate. The agreement between theoretical and experimental results, which has been obtained with no fitting procedure except from a tuning of the  $n^{++}$  and  $p^{++}$  doping levels, validates the proposed NEGF-DD coupled approach.

At present, NEGF has been coupled to the 1D Drift-diffusion 1D ANALYSIS D1ANA [24]. Future developments will deal with its application to the quasi-3D multiphysics simulation, in the framework of the Vcsel Electro-opto-thermal NUMerical Simulator VENUS [25].

#### ACKNOWLEDGMENTS

This work was supported in part by the U.S. Army Research Laboratory through the Collaborative Research Alliance (CRA) for MultiScale multidisciplinary Modeling of Electronic materials (MSME).

#### REFERENCES

- [1] W. Hofmann, *IEEE Photon. J.* **2**, 802 (2010).
- [2] S. Spiga, *et al.*, *J. Lightwave Technol.* **35**, 727 (2017).
- [3] A. Caliman, *et al.*, *Opt. Express* **24**, 16329 (2016).
- [4] M. Grupen, K. Hess, *IEEE J. Quantum Electron.* **34**, 120 (1998).
- [5] M. Streiff, A. Witzig, M. Pfeiffer, P. Royo, W. Fichtner, *IEEE J. Select. Topics Quantum Electron.* **9**, 879 (2003).
- [6] C. De Santi, *et al.*, *Nitride Semiconductor Light-Emitting Diodes*, J. J. Huang, H. C. Kuo, S.-C. Shen, eds. (Woodhead Publishing, Duxford, U.K., 2018), chap. 14, pp. 455–489, second edn.
- [7] A. P. Cédola, *et al.*, *Int. J. Photoenergy* **2018**, 7215843 (2018).
- [8] E. O. Kane, *J. Appl. Phys.* **32**, 83 (1961).
- [9] G. A. M. Hurx, D. B. M. Klaassen, M. P. G. Knuyvers, *IEEE Trans. Electron Devices* **39**, 331 (1992).
- [10] A. Schenk, *Solid-State Electron.* **36**, 19 (1993).
- [11] M. Jeong, P. M. Solomon, S. Laux, H.-S. P. Wong, D. Chidambarrao, *1998 IEEE International Electron Devices Meeting (IEDM '98)* (San Francisco, CA, USA, 1998), pp. 733–736.
- [12] D. Esseni, M. Pala, P. Palestri, C. Alper, T. Rollo, *Semiconductor Sci. Tech.* **32**, 083005 (2017).
- [13] M. Vallone, *et al.*, *J. Electron. Mater.* **44**, 3056 (2015).
- [14] N. Moulin, M. Amara, F. Mandorlo, M. Lemiti, *J. Appl. Phys.* **126**, 033105 (2019).
- [15] H.-Y. Wong, D. Dolgos, L. Smith, R. V. Mickevicius, *Microelectron. Reliability* **104**, 113552 (2020).
- [16] D. L. Scharfetter, H. K. Gummel, *IEEE Trans. Electron Devices* **ED-16**, 64 (1969).
- [17] G. Ghione, A. Benvenuti, *IEEE Trans. Antennas Propagation* **AP-45**, 443 (1997).
- [18] U. Aeberhard, R. H. Morf, *Phys. Rev. B* **77**, 125343 (2008).
- [19] F. Bertazzi, *et al.*, *Handbook of Optoelectronic Device Modeling and Simulation*, J. Piprek, ed. (CRC Press, Boca Raton, FL, 2017), chap. 2, pp. 35–80.
- [20] C. Rivas, *et al.*, *Appl. Phys. Lett.* **78**, 814 (2001).
- [21] W. Vandenberghe, B. Sorée, W. Magnus, M. V. Fischetti, *J. Appl. Phys.* **109**, 124503 (2011).
- [22] U. Aeberhard, *Phys. Rev. B* **87**, 081302 (2013).
- [23] U. Aeberhard, *IEEE J. Select. Topics Quantum Electron.* **19**, 4000411 (2013).
- [24] M. Calciati, A. Tibaldi, F. Bertazzi, M. Goano, P. Debernardi, *Semiconductor Sci. Tech.* **32**, 055007 (2017).
- [25] A. Tibaldi, F. Bertazzi, M. Goano, R. Michalzik, P. Debernardi, *IEEE J. Select. Topics Quantum Electron.* **25**, 1500212 (2019).